ASIAN JOURNAL OF PHARMACEUTICAL AND CLINICAL RESEARCH

INNOVARE ACADEMIC SCIENCES
Knowledge to Innovation

Vol 12, Issue 5, 2019

Online - 2455-3891
Print - 0974-2441

Research Article

A POTENT CYTOTOXICITY AND ANTIMICROBIAL ACTIVITY OF ZINC OXIDE NANOPARTICLES SYNTHESIZED BY LEAF OF *IPOMOEA PES-CAPRAE* (L.) R. BR.

RAMESH A*, SUNDARRAJ P, BALAMANI J

Department of Chemistry, Chikkanna Government Arts College, Tirupur, Tamil Nadu, India. Email: rammsc.perfect@gmail.com

Received: 01 February 2019, Revised and Accepted: 22 March 2019

ABSTRACT

Objective: The present study was conducted to investigate the cytotoxicity and antimicrobial activity of zinc oxide nanoparticles (ZnO NPs) synthesized as eco-friendly technique from the leaf extract of *Ipomoea pes-caprae* (L.) R. Br. against human lung adenocarcinoma (A549), brain tumor (U87) cells, and human pathogens *Salmonella typhi*, *Staphylococcus aureus*, *Klebsiella pneumonia*, *Pseudomonas aeruginosa,* and *Bacillus subtilis*.

Materials and Methods: The work was carried out with varying precursor (plant extract) volume to optimize the synthesis of ZnO NPs and it was confirmed by ultraviolet (UV)-visible spectroscopy, Fourier-transform infrared spectroscopy (FTIR), X-ray diffraction (XRD) analysis, scanning electron microscopy, and atomic force microscope (AFM) characterization techniques and evaluate its cytotoxicity activity by 3-(4,5-dimethyl-2-thiazolyl)-2,5-diphenyl--tetrazolium bromide assay method, antimicrobial activity by disk diffusion method.

Results: A peak at 320 nm with maximum intensity was observed at temperature of 80°C with pH of 8.0 in UV-visible spectroscopy confirmed the formation of ZnO NPs and we calculate the size of ZnO NPs from XRD data found as 15.8 nm. The FTIR analysis evaluated that the presence of different functional groups is carboxyl, amine, and phenolic compounds of leaves extract which are involved in the reduction of zinc ions and acts as capping the ZnO NPs. AFM microgram confirms that ZnO NPs were in nanorange and spherical in nature. The cytotoxicity activity of A549 and U87 cell lines treated with various concentrations of ZnO NPs showed a dose-dependent increase in cell inhibition and the half maximal inhibitory concentration value was calculated to be 7.8 µg/ml. The antibacterial activity of selected pathogens shows higher zone of inhibition.

Conclusion: The present study reveals that synthesized ZnO NPs capping with various bioactive compounds present in the leaf of *I. pes-caprae* show promising activity of cancer cell lines and antimicrobial agents; hence, further detailed study may lead to develop at a novel phytomedicine for the anticancer and antimicrobial drugs.

Keywords: *Ipomoea pes-caprae,* Zinc nanoparticles, A549 cell line, U87 cell line, Anticancer activity, Antimicrobial activity.

 DOI: http://dx.doi.org/10.22159/ajpcr.2019.v12i5.32318

INTRODUCTION

Recently, there is much focusing on natural products obtained from plants and herbal resources, *Ipomoea pes-caprae* consider as an example of phytocompounds richest resources. *I. pes-caprae* is used in flock medicine against inflammation and gastrointestinal disorder and as an analgesic agent [1]. *I. pes-caprae* is an ancient plant employed in the treatment of headache and various types of inflammation including jellyfish sting dermatitis [2]. In recent years, noble metal nanoparticles (NPs) have been the subjected of focused research due to their unique optical, electronic, mechanical, magnetic, and chemical properties that are significantly different from those of bulk materials [3]. Numerous approaches using plant extract have been used for the synthesis of metal NPs. The biosynthetic methodology employing plant extracts [4] has received much attention recently due to its simplicity, ecofriendliness, and economically viable nature, compared to the other existing methods such as using bacteria and fungi [5], and chemical [6] and physical methods used for synthesis of metal NPs. Zinc oxide NPs (ZnO NPs) have a tremendous potential in biological applications such as biological sensing [7], biological labeling, gene delivery, drug delivery [8], and nanomedicine along with its antibacterial [9], antifungal [10], acaricidal, pediculicidal, larvicidal [11], and antidiabetic activities [12]. ZnO NPs are known to be one of the multifunctional inorganic NPs with effective antibacterial activity [13]. Antibacterial and antifungal activities of ZnO NPs are observed even at very lower concentrations and the antifungal activity does not affect soil fertility compared to the conventional antifungal agents [14]. Based on literature, biosynthesis of ZnO NPs was reported using plant extracts including *Aloe vera* (leaf) [15], *Nephelium lappaceum* L. (fruit peel) [16], *Corymbia citriodora* (leaf) [17], *Polygala tenuifolia* (root) [18], *Trifolium pratense* (flower) [19], *Rosa canina* (fruit) [20], *Zingiber officinale* (rhizome) [21], *Eucalyptus globulus* (leaf) [22], and *Vitex trifolia* L. (leaf) [23]. Some reports show biosynthesized silver NPs from *I. pes-caprae* leaf extracts showed remarkable anticancer activity against liver cancer cells (A549) and human brain tumor cancer cell line (U87) and effective antibacterial activity [24].

In the present work, we tend to describe a green synthetic strategy to prepare ZnO NPs from leaves extract of *I. pes-caprae.* To confirm the presence of ZnO NPs, different characterization techniques were used and evaluate its cytotoxicity and antimicrobial activity of some selected cell lines and microbes.

MATERIALS AND METHODS

Chemicals, media, and cell line

Zinc acetate dihydrate ($Zn(CH_3COO)_2.2H_2O$) was purchased from Sigma-Aldrich, Mumbai, India. High pure double distilled water was used throughout the method. Both normal and Whatman No.1 filter paper were used for the filtration process. The A549 and U87 cell lines were obtained from the National Centre for Cell Sciences (NCCS), Pune.

Preparation of plant extracts

Whole plant of *I. pes-caprae* was collected from Manakudi coastal area, Kanyakumari district, Tamil Nadu, India. The well-cleansed leaves were cut into smaller pieces using a sterilized knife thereafter allowed to dry in a hot air oven for 24 h at 40°C. The dried, cut leaves were removed from the oven and cooled down to room temperature before grinding using a mechanical grinder. The powdered leaves were collected and

filtered using mesh to collect very fine powder. The fine powders were then packed in airtight bags and keep for future use. From the fine powder, 5 g was weighed in a conical flask, to which 100 ml of double distilled water was poured into it. The mixture was refluxed using hot plate heated around 60°C for 1 h by stirring continuously to avoid evaporation. The extract obtained was then filtered out using Whatman filter paper, and the collected extract was kept in cold condition for the future synthesis process.

Phytosynthesis of ZnO NPs

About 20 ml of the plant extract was heated at 50°C for 10 min and 50 ml of 91 mM of zinc acetate solution (1 gm of zinc acetate was dissolved in 50 ml of distilled water) was added dropwise to it under stirring. The reaction mixture became yellowish and cream-colored precipitate of zinc hydroxide was formed. The reaction mixture was left for 30 min for complete reduction to zinc hydroxide. Then, the precipitate was collected by centrifugation at 16,000 rpm for 10 min at 4°C. The precipitate was vacuum dried at 30°C and the pellet (ZnO NPs) was stored for further studies. Two other samples were prepared by varying the ratio of plant extract (10 ml and 30 ml) to zinc acetate (v/w) and were represented by the yield of ZnO, calculated using the following formula:

$$\text{Yield (\%)} = (\text{Experimental weight of ZnO} / \text{Theoretical weight of ZnO}) \times 100$$

Characterization of silver NPs

Ultraviolet (UV)-visible spectroscopy

The bioreduction of reaction mixture of the pure ZnO NPs was ascertained by observing the UV-visible spectroscopy at 200–800 nm using 1 ml of sample, compared with 1 ml of distilled water used as blank.

Fourier-transform infrared spectroscopy (FTIR)

To identify ZnO NPs associated biomolecules, the FTIR of powdered ZnO NPs was recorded on the Nicolet Avatar 660 FT-IR Spectroscopy using KBr pellets. To obtain better signal-to-noise ratio, 256 scans were taken in the range of 400–4000 cm^{-1} and the resolution was kept as 4 cm^{-1}.

X-ray diffraction (XRD)

The crystalline size and purity were characterized by X-ray diffractometer (Bruker D8 Advance) using Cu-Ka radiation of wavelength k= 1.541 A of synthesized ZnO NPs. The particle size of the prepared samples was determined using the Scherrer's equation as follows: $D \approx 0.9/\cos\theta$, where, D is the crystal size, k is the wavelength of X-ray, h is the Braggs angle in radians, and B is the full width at half maximum (FWHM) of the peak in radians.

Scanning electron microscopy (SEM)

CARL ZEISS EVO18 SEM machine was used to characterize the morphology of ZnO NPs. Thin films of the sample were prepared on a carbon-coated copper grid by simply dropping a very small amount of the sample on the grid, extra solution was removed using a blotting paper, and then, the film on the SEM grid could dry by putting it under a mercury lamp for 5 min. The photographs were captured in SEM mode at the desired magnification.

Atomic force microscope (AFM) analysis

The synthesized NPs were spreading on the glass slides then dried and subjected for characterization to find morphological and structural properties by AFM AGILENT-N9410A-5500.

Biological application

Antibacterial activity

The antibacterial activity of the ZnO NPs was evaluated against *Salmonella typhi*, *Staphylococcus aureus*, *Klebsiella pneumonia*, *Pseudomonas aeruginosa,* and *Bacillus subtilis* using agar well diffusion method. The antibacterial effect of ZnO NPs has been reported against Gram-positive and Gram-negative bacteria due to larger surface area and electrostatic interaction of NPs. Stock cultures were maintained at 4°C on nutrient agar slant. Active cultures for experiments were prepared by transferring a loop full of culture from the stock cultures into the test tubes containing nutrient broth that was incubated at 24 h at 37°C. Antibacterial activity of extracts was determined by agar disc diffusion method on Mueller-Hinton agar (MHA) medium. MHA medium is poured into the Petri plate. Once the medium was solidified, the inoculums were spread on the solid plates with sterile swab moistened with the bacterial suspension. Different concentrations of the sample were prepared (1000 µg, 750 µg, and 500 µg). 20 µl of sample from each concentration was taken and added into the sterile discs and air dried. Then, the sample loaded disc was placed on the MHA plates along with positive control and incubated at 37°C for 24 h, and the antimicrobial activity was determined by measuring the diameter of zone of inhibition.

Cytotoxicity studies

Liver cancer cells (A549), and human brain tumor cancer (U87) cell lines were purchased from NCCS, Pune, India. It was cultured in Dulbecco's modified Eagle's Medium (DMEM, HiMedia Laboratories, Mumbai, India), supplemented with 10% fetal bovine serum and 1% penicillin/streptomycin (HiMedia Laboratories, Mumbai, India). The cell lines were maintained at 5% CO_2 in CO_2 incubator. Cultures were examined using an inverted microscope to evaluate the quality of confluence and confirming the absence of bacterial and fungal contaminants.

3-(4,5-dimethyl-2-thiazolyl)-2,5-diphenyl-tetrazolium bromide (MTT) assay

To determine the cytotoxic effect of ZnO NPs synthesized from *I. pes-caprae* leaves extract, cell viability study was carried out with the MTT reduction assay. A549 and U87 cells (1×10^5/well) were plated in 24-well plates and incubated in 37°C with 5% CO_2 condition. After the cell reaches the confluence, the various concentrations of the ZnO NPs were added and incubated for 24 h. After incubation, the sample was removed from the well and washed with phosphate-buffered saline (pH 7.4) or DMEM without serum. 100 µl/well (5 mg/ml) of 0.5% MTT was added and incubated for 4 h. After incubation, 1 ml of dimethyl sulfoxide (DMSO) was added in all the wells. The absorbance at 570 nm was measured with UV spectrophotometer using DMSO as the blank. Measurements were performed and the concentration required for a 50% inhibition (half maximal inhibitory concentration [IC_{50}]) was determined graphically. The percentage of cell viability was calculated using the following formula:

$$\text{Percentage of cell viability} = \frac{\text{O.D of treated cells}}{\text{O.D of control cells}} \times 100$$

Graphs were plotted using the percentage of cell viability at Y-axis and concentration of the sample in X-axis. Cell control and sample control are included in each assay to compare the full cell viability assessments.

RESULTS AND DISCUSSION

Effect of plant extract concentration on ZnO NP synthesis

Concentration of plant extract plays a key role in the synthesis of ZnO NPs. It has been observed that the ratio of plant extract to zinc acetate 20 ml/gm (i.e., 1 gm of zinc acetate in 20 ml of plant extract) was optimal concentration for the synthesis of ZnO NPs which gives yield 95%. Insufficient amount of bioactive compound present in 10 ml/gm of zinc acetate lowers the yield of ZnO NPs gives 70%, whereas 30 ml/gm of zinc acetate yield 95% nearly same amounts of ZnO NPs that yield in 20 ml/gm (Fig. 1). That means, the number of bioactive compounds present in case of 20 ml/gm was sufficient to reduce all Zn^{2+} ions present in the reaction mixture.

Characterization of synthesized ZnO NPs

UV-visible spectrum

UV-visible spectroscopy used to identify the synthesis of ZnO NPs (Fig. 2) represents the formation of ZnO NPs. Freshly prepared ZnO suspensions in plant extract exhibit a strong absorption at 320 nm in the UV region. This surface plasmon resonance band undergoes a red or blue shift, depending on the quantum size effects. The absorbance of ZnO NPs depends on their shape and size. The plant extract reacts with Zn^{2+} ions reduces the precursor solution and formation of NPs monitored by UV-visible spectroscopy.

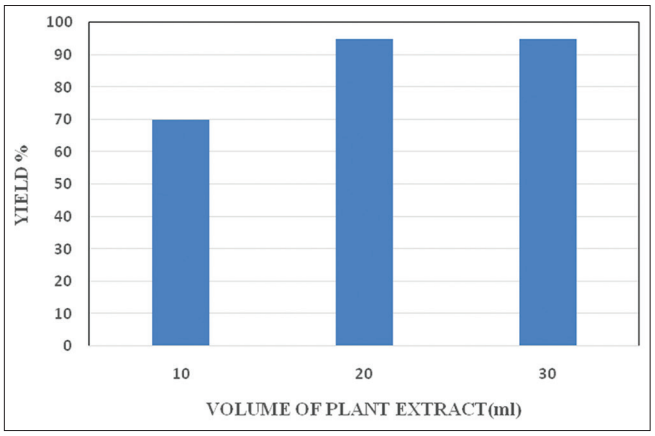

Fig. 1: Effect of plant extract concentration in synthesis of zinc oxide nanoparticles

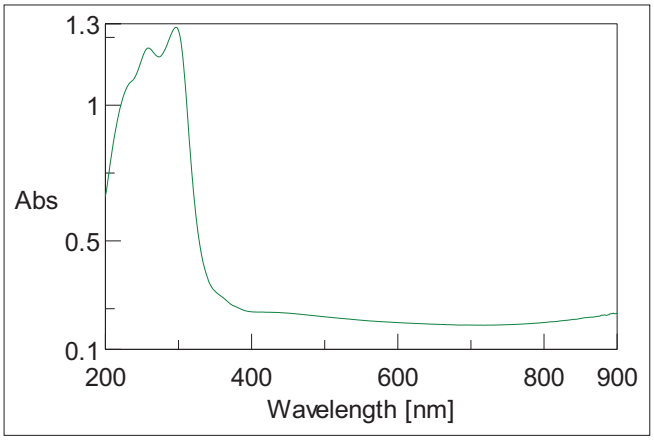

Fig. 2: Ultraviolet-visible absorption spectrum of zinc oxide nanoparticles synthesized from *Ipomoea pes-caprae* leaves extract

FTIR analysis

The FTIR spectrum of *I. pes-caprae* leaves extract and synthesized ZnO NPs (Fig. 3) showed strong IR bands characteristic of carboxylic acids (1030 cm^{-1}), amines (1622 cm^{-1}), alkanes (2923 and 2853 cm^{-1}), O-H carboxylic acids (2362 cm^{-1}), and hydrogen bonded alcohols (3416 cm^{-1}) functional groups. The band at 3424.94 cm^{-1} that corresponds to normal "polymeric" OH stretching mode. The peak at 2923cm^{-1} associated to the methylene C-H asymmetric and symmetric stretching mode. The peak at 2362 cm^{-1} indicates the symmetric stretching of alkanes and the peak at 1622 cm^{-1} attributed to the C=O stretching mode of ketones. The peak at 1384 cm^{-1} corresponds to the N=O stretching of nitro groups of leaves extract. Here, we confirm the modulated transmittance percentage of ketone, polymeric OH compounds, and amine groups play a key role for the bioreduction of Zn^{2+} to ZnO NPs. The FTIR analysis strongly supported the capping behavior of bioreduced ZnO NPs synthesized by *I. pes-caprae* leaves extracts which, in turn, imparted the high stability of the synthesized NPs.

XRD analysis

The XRD spectra of *I. pes-caprae* leaf aqueous extract mediated ZnO NPs are shown in Fig. 4. The prominent peaks corresponding to the diffraction planes (100), (002), (101), (012), (102), (110), (103), (200), (112), (201), and (202) agreed well with the JCPDS Card No. 36-1451, confirming the hexagonal wurtzite structure of the ZnO NPs. The strong intensity and broadened diffraction peaks clearly indicate that the ZnO NPs are highly crystalline in nature. Similar results are obtained by Yu *et al.* [25]. The average particle size (D) of synthesized NPs was calculated using the well-known Scherrer formula D=0.9 k/b cos θ, where, k is the wavelength of X-ray source (Cu-Ka line – 0.1541 nm), b is the FWHM in radians, and h is Bragg's diffraction angle. The calculated value of D was 15.8 nm.

SEM

The shape, structure, and size of the ZnO NP synthesized using leaf extracts of *I. pes-caprae* was determined by the SEM analysis (Fig. 5) and an average size of about 27 nm was seen in the ZnO NP. The previous studies showed that the ZnO NPs were in the range of 37 nm and these were in accordance to our present study [26].

AFM

The AFM of 2D and 3D result images that shown in Fig. 6 showed the morphological and structural characterization of green synthesized

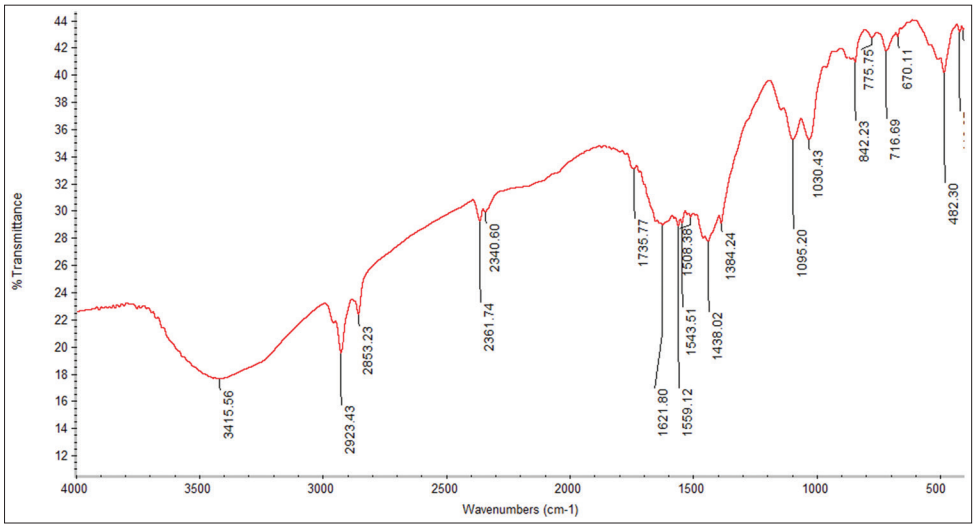

Fig. 3: Fourier-transform infrared spectroscopy spectrum of synthesized zinc oxide nanoparticles

Table 1: Antibacterial activity of the ZnO NPs synthesized by *I. pes-caprae* leaves extract

Bacterium name	Zone of inhibition (mm)			
	Control (ampicillin) 1000 µg/mL	1000 µg/ml	750 µg/ml	500 µg/ml
Staphylococcus aureus	21	11	9	9
Bacillus subtilis	23	12	9	8
Klebsiella pneumoniae	18	13	10	9
Salmonella typhi	47	20	11	9
Pseudomonas aeruginosa	25	15	11	10

I. pes-caprae: Ipomoea pes-caprae, ZnO NPs: Zinc oxide nanoparticles

Table 2: Cytotoxicity activity of the ZnO NPs synthesized by *I. pes-caprae* leaves extract

S. No.	Concentration (µg/ml)	Dilution	Absorbance (O.D)		Cell viability (%)	
			A549	U87	A549	U87
1	1000	Neat	0.116	0.082	11.98	11.76
2	500	1:1	0.162	0.109	16.73	15.63
3	250	1:2	0.211	0.135	21.79	19.36
4	125	1:4	0.264	0.172	27.27	24.67
5	62.5	1:8	0.326	0.212	33.67	30.41
6	31.2	1:16	0.389	0.246	40.18	35.29
7	15.6	1:32	0.453	0.286	46.79	41.03
8	7.8	1:64	0.512	0.338	52.89	48.49
9	Cell control		0.968	0.697	100	100

I. pes-caprae: Ipomoea pes-caprae, ZnO NPs: Zinc oxide nanoparticles

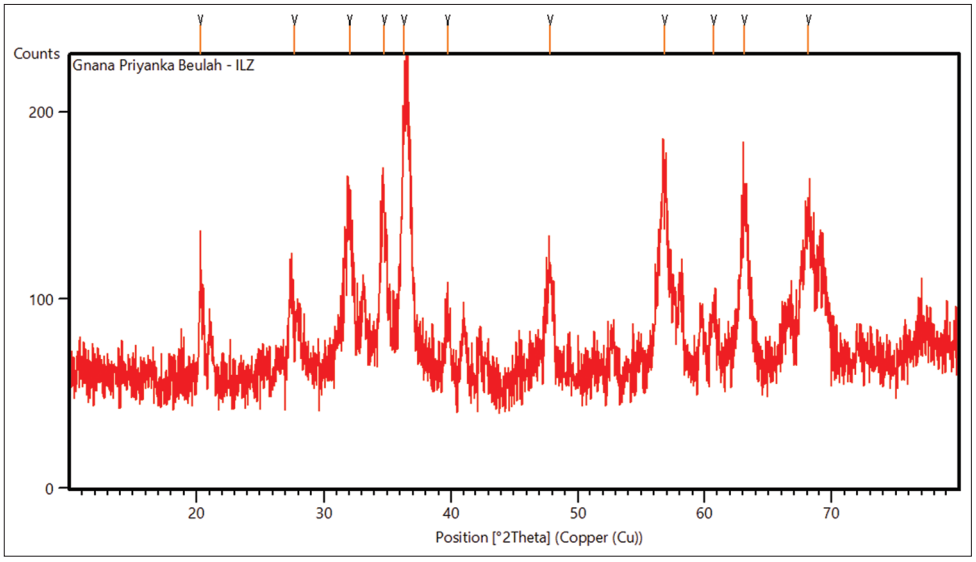

Fig. 4: X-ray diffraction spectra of zinc oxide nanoparticles using *Ipomoea pes-caprae* leaves aqueous extract

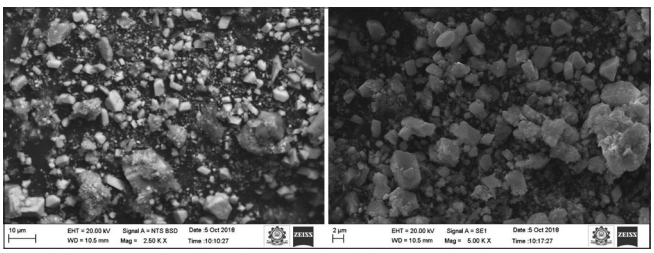

Fig. 5: Scanning electron microscopy images of zinc oxide nanoparticles using *Ipomoea pes-caprae* leaves extract

ZnO NPs by *I. pes-caprae* leaves extract with average diameter of 40 nm. From the figure concluded that NPs are equal in size and their morphology also rough in nature cubical in shape.

Biological applications of ZnO NPs

Antibacterial activity

Synthesized ZnO NPs were analyzed by disk diffusion method using selected organisms such as *S. typhi*, *S. aureus*, *K. pneumonia*, *P. aeruginosa,* and *B. Subtilis* is shown in Fig.7. As the concentration of ZnO NPs increases, the zone of inhibition also increased against the bacteria strain is shown in Table 1. ZnO NPs synthesized from leaves extract exhibited significant activity against *S. typhi* and *P. aeruginosa* with zone of inhibition 20 and 15 mm is shown in Fig.8. This proves that the ZnO NPs synthesized by the simple solution method may be used for microbial activity study.

Finally, the current study clearly indicates that the synthesized ZnO NPs exhibit the zone of inhibition have high value obtained at Gram-negative organisms of *S. typhi* and *P. aeruginosa*. These plant-mediated ZnO NPs show high antibacterial activity which may be used in textiles coatings and wood flooring as antibacterial agents.

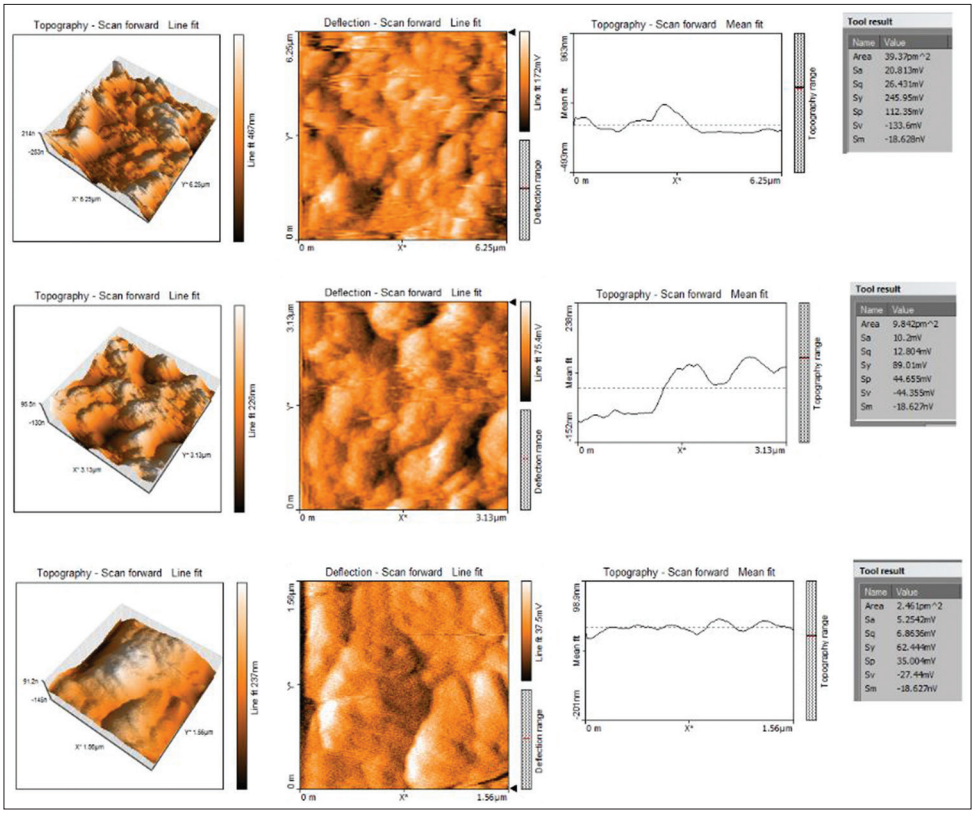

Fig. 6: Atomic force microscope images of zinc oxide nanoparticles synthesized by *Ipomoea pes-caprae* leaf extract

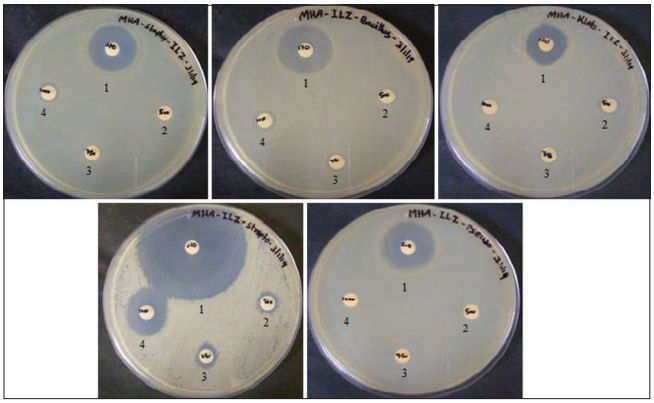

Fig. 7: The antibacterial activity of zinc oxide nanoparticles from leaves extract in (a) *Staphylococcus aureus*, (b) *Bacillus subtilis* (c) *Klebsiella pneumonia*, (d) *Salmonella typhi*, (e) *Pseudomonas aeruginosa*, at various concentrations ([1] Positive control, [2] 500 µg/ml, [3] 750 µg/ml, and [4] 1000 µg/ml)

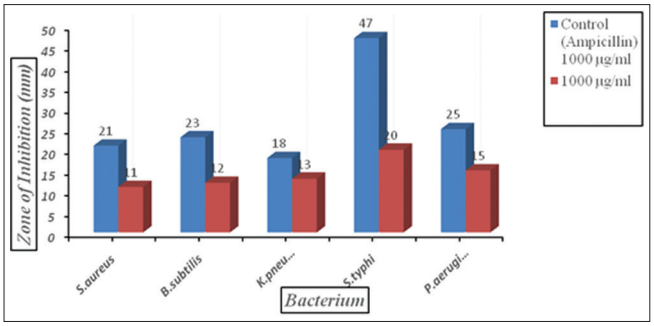

Fig. 8: Effect of antibacterial activity of zinc oxide nanoparticles from leaves extract with positive control

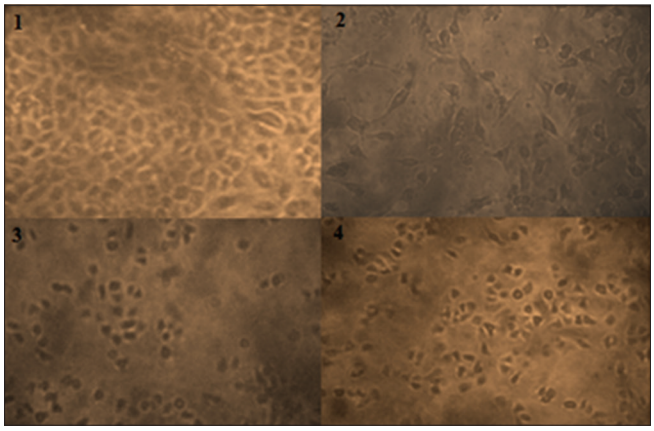

Fig. 9: Anticancer activity of zinc oxide nanoparticles from leaves extract of *Ipomoea pes-caprae* in A549 cell line ([1] Normal A549 cell line, [2] Toxicity – 1000 µg/ml, [3] Toxicity – 62.5 µg/ml, and [4] Toxicity – 7.8 µg/ml)

Cytotoxicity analysis

The cytotoxicity of the ZnO NPs synthesized from *I. pes-caprae* leaves extract was studied against the A549 (Fig. 9) and U87 (Fig. 10) cell line by MTT assay. The cytotoxicity effect of cancer cell was studied at different concentrations (1000 µg/ml–7.8 µg/ml) is shown in Table 2. The IC_{50} value of the phyto-mediated ZnO NPs of leaves extract at the cell viability of 52.9% (Fig. 11) against A549 cells was observed at 7.8 µg/ml and for U87 cells was observed as 48.5% at the concentration of 7.8 µg/ml (Fig. 12). This study shows that the minimum dose showed significant anticancer activity. Some reports exhibit that ZnO NPs may stimulate reactive oxygen species and effect in damage cellular components which lead to cell death [27]. Some reports show that ZnO NPs were induced greater cytotoxicity in the colon, liver, lung, and skin cells at higher concentrations of 100 and 300 µg/ml significantly [28].

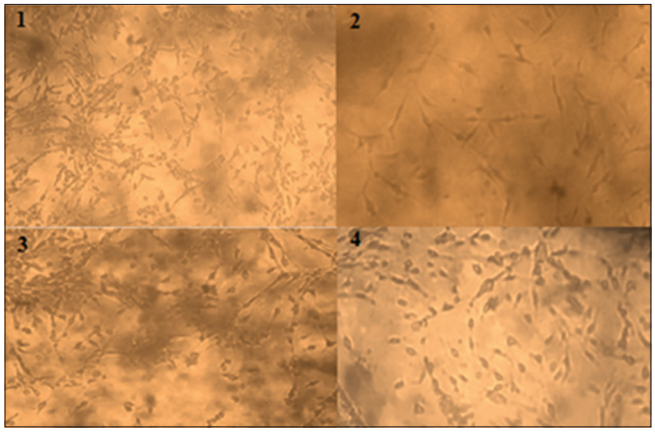

Fig. 10: Anticancer activity of zinc oxide nanoparticles from leaves extract of *Ipomoea pes-caprae* in U87 cell line ([1] Normal U87 cell line, [2] Toxicity – 1000 µg/ml, [3] Toxicity – 62.5 µg/ml, and [4] Toxicity – 7.8 µg/ml)

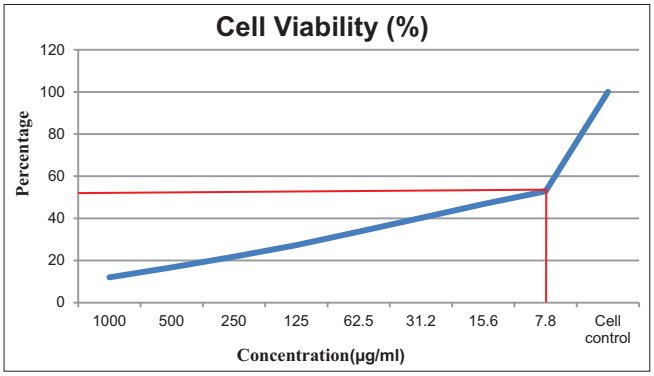

Fig. 11: Half maximal inhibitory concentration value of zinc oxide nanoparticles from leaves extract against A549 cell line

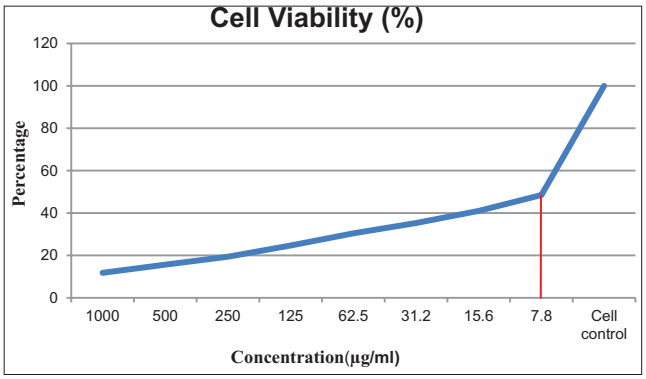

Fig. 12: Half maximal inhibitory concentration value of zinc oxide nanoparticles from leaves extract against U87 cell line

CONCLUSION

We report a simple straight forward, facile, inexpensive, eco-friendly, and green synthesis of ZnO NPs from *I. pes-caprae* leaves in aqueous medium without employing man-made chemicals. The UV-visible spectroscopy and FT-IR analysis are confirmed the preliminary confirmation of the formation of ZnO NPs. AFM image showed cubical shape with an average particle size of 40 nm. The biosynthesized ZnO NPs from *I. pes-caprae* leaf extracts showed remarkable anticancer activity against liver cancer cells (A549) and human brain tumor cancer cell line (U87) and effective antibacterial activity. From the study, it can be concluded that the ZnO NPs synthesized using plant possess high anticancer and antibacterial activity which further suggested the potential therapeutic use of these NPs.

ACKNOWLEDGMENT

We would like to acknowledge Dr. I Seethalakshmi, Director, Life Teck Research Centre, Chennai, for his professional helping hand in biological studies.

AUTHORS' CONTRIBUTIONS

The present work selection, procurement, synthesis, and biological studies were done by Mr. A Ramesh and wrote the manuscript under the supervision of Prof. J Balamani.

CONFLICTS OF INTEREST

The authors declare that there were no conflicts of interest.

REFERENCES

1. Souza MM, Madeira A, Berti C, Krogh R, Yunes RA, Cechinel-Filho V. Antinociceptive properties of the methanolic extract obtained from *Ipomoea pes-caprae* (L.)R. Br J Ethnopharmacol 2000;69:85-90.
2. Bandaranayake WM. Bioactivities, bioactive compounds and chemical constituents of mangrove plants. Wetl Ecol Manag 2002;10:421-52.
3. Gavhane AJ, Padmanabhan P, Kamble SP, Jangle SN. Synthesis of silver nanoparticles using extract of neem leaf and triphala and evaluation of their antimicrobial activities. Int J Pharm Bio Sci 2012;42:20-31.
4. Dhanalakshmi T, Rajendran S. Synthesis of silver nanoparticles using *Tridax procumbens* and its antimicrobial activity. Sch Res Libr Arch Appl Sci Res 2012;4:1289-93.
5. Oza G, Pandey S, Shah R, Sharon M. Extracellular fabrication of silver nanoparticles using *Pseudomonas aeruginosa* and its antimicrobial assay. Pelagia Res Libr Adv Appl Sci Res 2012;3:1776-83.
6. El-Kheshen AA, El-Rab SF. Effect of reducing and protecting agents on size of silver nanoparticles and their anti-bacterial activity. Der Pharm Chem 2012;4:55-63.
7. Yoon SH, Kim DJ. Fabrication and Characterization of ZnO Films for Biological Sensor Application of FPW Device. Applications of Ferroelectrics. 15th IEEE International Symposium on the July 30; 2006. p. 322-5.
8. Rasmussen JW, Martinez E, Louka P, Wingett DG. Zinc oxide nanoparticles for selective destruction of tumor cells and potential for drug delivery applications. Expert Opin Drug Deliv 2010;7:1063-77.
9. Applerot G, Lipovsky A, Dror R, Perkas N. Enhanced antibacterial activity of nanocrystalline ZnO due to increased ROS-mediated cell injury. Adv Funct Mater 2009;19:842-52.
10. Sharmaa D, Rajputa J, Kaitha BS, Kaurb M. Synthesis of ZnO nanoparticles and study of their antibacterial and antifungal properties. Thin Solid Films 2010;519:1224-9.
11. Kirthi AV, Rahuman AA, Rajakumar G, Marimuthu S, Santhoshkumar T, Jayaseelan C, *et al.* Acaricidal, pediculocidal and larvicidal activity of synthesized znO nanoparticles using wet chemical route against blood feeding parasites. Parasitol Res 2011;109:461-72.
12. Alkaladi A, Abdelazim AM, Afifi M. Antidiabetic activity of zinc oxide and silver nanoparticles on streptozotocin-induced diabetic rats. Int J Mol Sci 2014;15:2015-23.
13. Gunalana S, Sivaraja R, Rajendranb V. Green synthesized ZnO nanoparticles against bacterial and fungal pathogens. Prog Nat Sci Mater Int 2012;22:693-700.
14. Feris K, Otto C, Tinker J, Wingett D, Punnoose A, Thurber A, *et al.* Electrostatic interactions affect nanoparticle-mediated toxicity to gram-negative bacterium *Pseudomonas aeruginosa* PAO1. Langmuir 2010;26:4429-36.
15. Ali K, Dwivedi S, Azam A, Saquib Q, Al-Said MS, Alkhedhairy A, *et al. Aloe vera* extract functionalized zinc oxide nanoparticles as nanoantibiotics against multi-drug resistant clinical bacterial isolates. J Colloid Interface Sci 2016;472:145-56.
16. Karnan T, Stanly AS. Biosynthesis of ZnO nanoparticles using rambutan (*Nephelium lappaceum* L.) peel extract and their photocatalytic activity on methyl orange dye. J Mol Struct 2016;1125:358-65.
17. Zheng Y, Fu L, Han F, Wang A, Cai W, Yu J, *et al.* Green biosynthesis and characterization of zinc oxide nanoparticles using *Corymbia citriodora* leaf extract and their photocatalytic activity. Green Chem Lett Rev 2015;8:59-63.

18. Nagajyothi PC, Ju S, Jun I, Sreekanth TV, Joong K, Mook H. Antioxidant and anti-inflammatory activities of zinc oxide nanoparticles synthesized using *Polygala tenuifolia* root extract. J Photochem Photobiol B 2015;146:10-7.
19. Dobrucka R, Długaszewska J. Biosynthesis and antibacterial activity of ZnO nanoparticles using *Trifolium pratense* flower extract. Saudi J Biol Sci 2001;23:517-23.
20. Jafarirad S, Mehrabi M, Divband B, Kosari-NasabM. Biofabrication of zinc oxide nanoparticles using fruit extract of *Rosa canina* and their toxic potential against bacteria: A mechanistic approach. Mater Sci Eng C 2016;59:296-302.
21. Anbuvannan M, Ramesh M, Viruthagiri G, Shanmugam N, Kannadasan N. Synthesis, characterization and photocatalytic activity of ZnO nanoparticles prepared by biological method. Spectrochim Acta Part A 2015;143:304-8.
22. Balaji S, Kumar MB. Facile green synthesis of zinc oxide nanoparticles by *Eucalyptus globulus* and their photocatalytic and antioxidant activity. Adv Powder Technol 2017;28:785-97.
23. Elumalai K, Velmurugan S, Ravi S, Kathiravan V, Raj GA. Bio-approach: Plant mediated synthesis of ZnO nanoparticles and their catalytic reduction of methylene blue and antimicrobial activity. Soc Powder Technol Jpn 2015;26:1639-51.
24. Ramesh A, Sundarraj P, Balamani J. Characterization and biological evaluation of silver nanoparticles synthesized by leaf extracts of *Ipomoea pes-caprae* (L) R. BR. JETIR 2018;5:510-20.
25. Yu ZJ, Kumar MR, Sun DL, Wang LT, Hong RY. Large scale production of hexagonal ZnO nanoparticles using PVP as a surfactant. Mater Lett 2016;166:284-7.
26. Raj LF, Jayalakshmy E. A biogenic approach for the synthesis and characterization of zinc oxide nanoparticles produced by *Tinospora cordifolia*. Int J Pharm Pharm Sci 2015;7:384-6.
27. Jacob JP, Finub S, Narayanan A. Synthesis of silver nanoparticles using *Piper longum* leaf extracts and its cytotoxic activity against Hep-2 cell line. Colloids Surf B Biointerfaces 2012;91:212-6.
28. Durgaiah G, Harikiran L, Narsimha RY. Cytotoxicity evaluation of titanium and zinc oxide nanoparticles on human cell lines. Int J Pharm Pharm Sci 2017;11:240-6.